Proceedings of the ASME 2013 Dynamic Systems and Control Conference
DSCC2013
October 21-23, 2013, Palo Alto, California, USA

DSCC2013-3875

DESIGN AND MODELING OF A SERIES ELASTIC ELEMENT FOR SNAKE ROBOTS

David Rollinson, Steven Ford, Ben Brown and Howie Choset
The Robotics Institute
Carnegie Mellon University
Pittsburgh, Pennsylvania 15213
Email: drollins@cs.cmu.edu

ABSTRACT

In this work, we detail the design, fabrication, and initial modeling of a compact, high-strength series elastic element designed for use in snake robots. The spring achieves its elasticity by torsionally shearing a rubber elastomer that is bonded to two rigid plates, and it is able to achieve mechanical compliance and energy storage that is an order of magnitude greater than traditional springs. Its novel design features a tapered conical cross-section that creates uniform shear stress in the rubber, improving the ultimate strength. Tests show that the torque-displacement profile of these springs is approximately linear, and initial results are reported on creating more accurate models that account for the element's hysteresis and viscoelastic properties. Low-bandwidth force control is demonstrated by measuring the element's torsional deflection to estimate the torque output of one of our snake robot modules.

INTRODUCTION

Snake robots are a type of hyper-redundant mechanism [1] that consist of a series chain of actuated links that enable snake-like locomotion. Their small cross section and wide range of motions allow them to navigate many diverse environments, such as rough ground, channels, pipes, poles, and trees. This makes snake robots applicable to a diverse set of tasks such as urban search and rescue, mine rescue, industrial inspection, and reconnaissance. The snake robots developed by our group lack active or passive wheels and rely only on their internal shape changes, created by position-controlled joints, to locomote [2].

Our snake robots are similar to most other mobile robots in that they rely on highly-geared electric motors for actuation, providing large torques at slow speeds. The modules of our latest robot use a brushed DC motor and a 400:1 gear train to produce peak torques of over 2.7 N-m and a maximum speed of 30 rpm. While this design makes the robot extremely capable of executing its commanded motions, the stiffness of the actuators makes sensing contact with the environment difficult.

(a) Series Elastic Spring

(b) Cross-Section

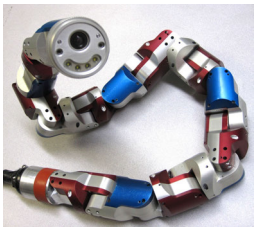

(c) *Unified Snake* Robot

(d) *Unified Snake* Module

Figure 1: Photo (upper left) and cross-section (upper right) of the bonded rubber series elastic element in this paper. The rubber is sheared torsionally about the element's central axis. The element is 25mm in diameter, 5mm thick, and weighs just under 5 grams. The softest springs can exert 8 N-m of torque and can withstand +/- 90° of rotational displacement. These elastic elements have been integrated into Carnegie Mellon's *Unified Snake* robot (bottom).

Theoretically, each module can estimate its output torque by measuring the current drawn by its motor, but in practice this is very difficult. Nonlinear effects like the friction, stiction, and reflected inertia of the gear train frequently cause the measured current to be significantly different from the actual torque at the output hub of the module. Adding series elasticity to our modules has the potential to mitigate these problems [3] as well as provide an easy and accurate estimate of the actuator's output torque, assuming the actuator has a relatively linear spring constant.

However, incorporating series elasticity into such a high-performance robot is not a trivial task. In order to be used in our snake robots, the series elastic element needs to have excellent energy storage and ultimate strength, fit in an extremely small design space, and be able to be manufactured reliably in large quantities (our lab currently has 60 snake modules). This work details the design, fabrication, and modeling of a high-performance series elastic element that torsionally shears rubber between two rigid plates. We show that this design meets all of the above design criteria, and that the spring's characteristics can be modeled well enough to enable accurate torque sensing in future robots.

PRIOR WORK

Prior work in snake robots begins with Hirose's pioneering work with the Active Cord Mechanism (ACM) [4]. The snake robots developed by our lab share many of the design characteristics of the ACM and similar snake robots [5], as well as characteristics of reconfigurable modular robots [6].

Outside of snake robots, there is a long history of series elastic actuation. Almost two decades ago Pratt and Williamson proposed series elasticity as a way of achieving actuator compliance and low-bandwidth force control [3]. Since then, work in series elastic actuator design and control has been primarily focused on legged locomotion [7–9].

Prior work in the design of rotary series elastic elements typically use steel torsion springs [10, 11] or fiberglass plates [8]. The custom torsion springs used for compliance and force sensing in the Robonaut 2 [11] are of a similar overall form factor to our design, but those springs have an order of magnitude less energy density, due to their use of a custom-machined steel profile rather than a sheared rubber element.

MECHANISM DESIGN

Since space and weight are extremely constrained in our snake robots, the material choice for the elastic element is important. Table 1 shows the specific energy of various materials in terms of both mass and volume [12]. Commercially available springs are commonly made out of fiberglass and steel because of those material's high energy recovery and linearity in spring stiffness. Although rubber has significantly higher specific energy than other materials, it is often avoided as a spring material because of its non-linear stiffness and hysteresis.

Material	Specific Energy (mass)	Energy Density (volume)
Steel	140 $\frac{J}{kg}$	1 $\frac{J}{cm^3}$
Fiberglass	770 $\frac{J}{kg}$	1.5 $\frac{J}{cm^3}$
Rubber	5200 $\frac{J}{kg}$	5 $\frac{J}{cm^3}$

Table 1: The specific energy and energy density of commonly used spring materials. By both weight and volume, rubber has by far the greatest specific energy [12].

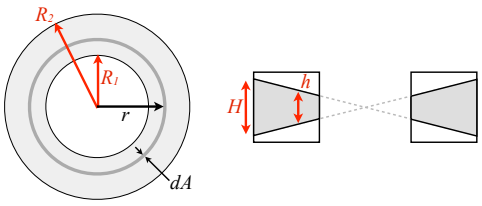

Figure 2: A diagram of the top view (left) and cross-section (right) of the conical tapered spring.

Tapered Design

Initial prototypes of the spring had a flat layer of rubber between the top and bottom plates. To maximize the ultimate load of the rubber inside the element, the cross-section of the element was later designed with a conical taper that intersects at the center of the spring, as shown in Fig. 2. This taper generates uniform shear stress across the entirety of the rubber, as opposed to a flat cross section where the periphery of the rubber is stressed more. Since the maximum shear stress in rubber is what limits the ultimate strength of the spring, designing the spring to uniform shear stress maximizes its ultimate strength.

The amount by which a tapered conical spring design increases the stiffness and strength of the spring can be calculated by integrating the spring's internal shear forces [13]. The torque T generated by the spring is a function of the shear stress τ integrated over differential rings of radius r

$$T = \int r\tau(r)\,(2\pi r\,dr). \tag{1}$$

As an approximation, we assume the shear stress is proportional to the rubber's shear modulus G, the spring's rotational displacement θ, the distance from the center of the spring r, and the thickness of the rubber h

$$\tau(r) = \frac{G\theta r}{h}. \tag{2}$$

Substituting into (1) and integrating from the spring's inner radius R_1 to its outer radius R_2 yields

$$T = 2\pi G\theta \int_{R_1}^{R_2} \frac{r^3}{h(r)}dr. \tag{3}$$

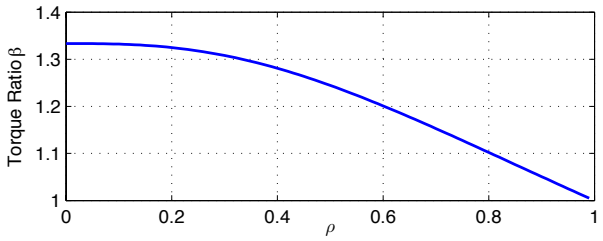

Figure 3: The ratio of increased stiffness and ultimate strength of a tapered cross-section elastic member compared to one with a flat cross-section for a range of ratios of inner and outer radii of the spring.

For a spring with a flat cross-section, the rubber has uniform thickness, H, throughout its radius

$$T_{\text{flat}} = \frac{\pi G\theta}{2H}(R_2^4 - R_1^4). \tag{4}$$

For the conical taper cross-section, the rubber thickness increases linearly with increasing spring radius

$$T_{\text{taper}} = \frac{2\pi R_2 G\theta}{3H}(R_2^3 - R_1^3). \tag{5}$$

To calculate the amount of increase in failure torque in the tapered spring compared to the flat spring, we take the ratio of (4) and (5) and express the result in terms of the ratios of the inner and outer radii of the spring

$$\rho = \frac{R_1}{R_2} \tag{6}$$

$$\beta = \frac{T_{\text{taper}}}{T_{\text{flat}}} = \frac{4(1-\rho^3)}{3(1-\rho^4)}. \tag{7}$$

This torque ratio β is greater than 1 for all $R_1 < R_2$. A plot of the torque ratio as a function of the ratio of inner and outer spring radius is shown in Fig. 3. For the springs presented in this paper $\rho = 0.6$, yielding a theoretical improvement in ultimate load and energy storage of 20% by using a tapered conical cross-section compared to a flat cross-section.

Manufacturing and Molding

For the most recent iteration of springs, we engaged a professional rubber molding company to mold neoprene and natural rubber to conical steel plates (Fig. 1). To test the maximum compliance that can be afforded by this spring design, we chose to have a set of springs fabricated with the softest durometer rubber available. We ordered and tested 3 different rubbers: 40A durometer neoprene, 40A durometer natural rubber, and 50A durometer natural rubber.

MODELING

To load test the springs, we built a small torque-sensing test rig. Our goals for testing were to determine the ultimate strength of various spring designs and rubber types, to characterize the linearity of various spring designs, and to make initial attempts to model hysteresis and other non-linear effects of the springs' torque-displacement curves.

	Neo 40A	**NR 40A**	**NR 50A**
Linear Model Error	8.9%	9.1%	5.5%
Hysteresis Model Error	5.1%	8.6%	2.6%
Spring Constant (N-m / °)	.055	.059	.101

Table 2: The average error and approximate spring constants for the 3 different rubber materials in the conical taper springs.

Overall, the rubber springs were surprisingly linear (Fig. 4), with the caveat that the spring constant softened after initial load cycling. This softening effect, known as the Mullins effect, is a well-documented phenomenon in most rubber elastomers [14]. Linear spring constants were fit to torque displacement data for all 3 springs after they had been initially load cycled. The best-fit spring constants and their average errors are presented in Table 2.

Modeling hysteresis was attempted using a model similar to a *viscoplastic material model* [14]. This physical model approximates the rubber as three parallel elements: a linear spring, a linear damper, and a frictional element with a series spring. Each of these elements has coefficients that are fit by optimizing the average squared error of the predicted model torque compared the actual spring torques measured by our test rig. Matlab's `fminsearch` optimizer was used to fit the parameters.

There are five parameters to be identified in this model: a spring coefficient, a viscous damping coefficient, a coefficient of friction of the frictional element, a yield force of the frictional element, and a spring coefficient in series with the frictional element. Figure 5 shows the predicted torque-displacement curve from this model along with the actual torque-displacement curve for the 40A durometer neoprene spring.

EXPERIMENTS AND VALIDATION

The elastic elements using 50A natural rubber have been integrated into one of our lab's snake robots (Fig. 1c). While we are unable to measure the deflection of the spring in the modules, we have been endurance testing them in the everyday use of our robot. No failures due to fatigue have occurred in the 19 retrofitted modules in over 6 months of use. Other tests to characterize the springs have been performed on a test jig.

Ultimate Strength

The molded springs that we tested to failure were 50A natural rubber, and had an ultimate strength of approximately 8 N-m at over 60° of displacement. Assuming a linear spring constant, the springs are storing approximately 6 J of energy. Since there is only 1.8 g of rubber in the spring, the rubber is theoretically

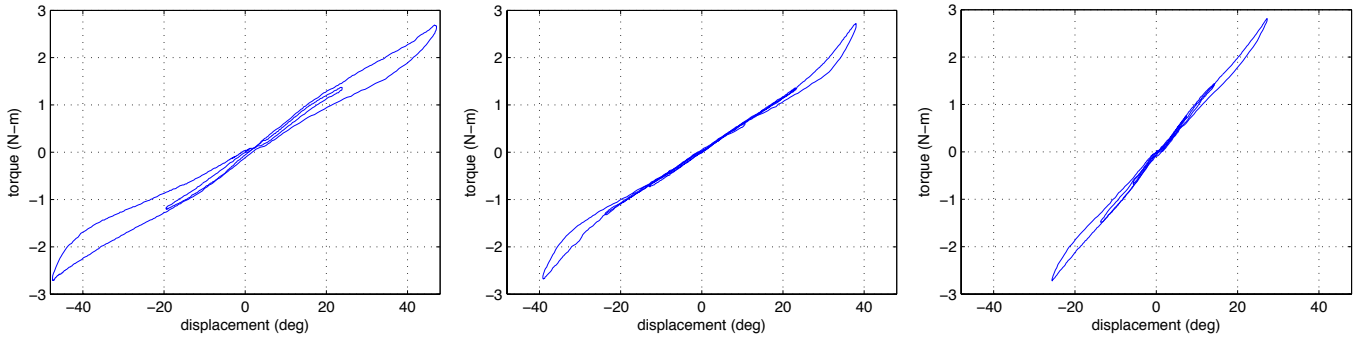

(a) Neoprene - 40A Durometer (b) Natural Rubber - 40A Durometer (c) Natural Rubber - 50A Durometer

Figure 4: A comparison for torque-displacement profiles for 3 different spring materials. The neoprene shows the most hysteresis and the lowest stiffness. The natural rubber springs have significantly less hysteresis. All of the the springs are approximately linear over a +/- 2.6 N-m torque range. The springs were cycled 3 times in increasing torque from from +/- .7 N-m to +/-2.6 N-m.

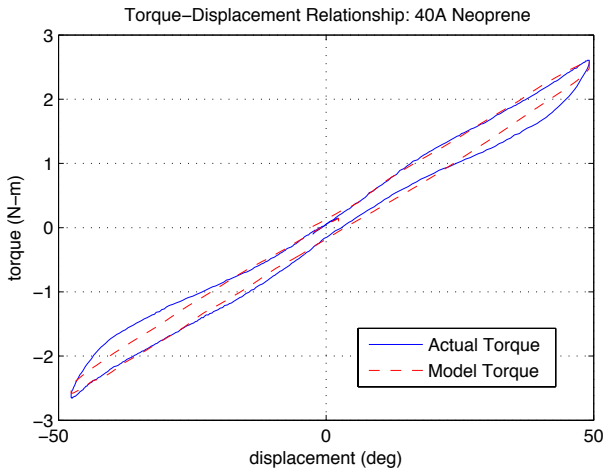

Figure 5: The actual (blue solid line) and modeled (red dashed line) torque-displacement curves for the 40A durometer neoprene spring, which exhibited the most hysteresis of the springs we tested. The spring was cycled through a torque of +/-2.6 N-m (2 ft-lbs).

exhibiting a specific energy density of approximately 3,000 J / kg, on the order of what can reasonably be expected for rubber (Table 1).

Force Control

As an initial proof of concept, we implemented a simple torque controller, using one of our snake robot modules and a molded 40 durometer natural rubber series elastic element. The module and spring were attached to a test rig that measured the output torque of the module and the absolute displacement of the spring. The torque was measured with a load cell that was attached to a lever arm that could be pivoted by hand. The robot module was commanded to exert a constant torque of 1.3 N-m, based on the spring's deflection and a linear spring constant, while the position of the lever arm was varied by hand. The feedback loop on estimated torque ran at approximately 17 Hz. The results of one of these tests is shown in Fig. 6.

While the module did a relatively poor job of tracking the commanded force, the estimated torque based on spring deflection was accurate to within 5%. The problems with using motor current to estimate force are also apparent in Fig. 6. In particular, stiction in the gear train causes the motor current to repeatedly drop to zero even though the module is actually exerting a significant torque.

CONCLUSIONS AND FUTURE WORK

We have presented a novel design for a rubber-based series elastic actuator. This design provides significant elasticity in an extremely small and flexible form factor. The use of bonded rubber element in torsional shear provides a surprisingly linear spring constant, even at torques of 2.6 N-m and angular displacements of 45°. The spring's tapered conical cross-section adds approximately 20% to its ultimate strength, compared to an initial flat cross-section design.

Strength and fatigue tests indicate that this spring design will allow mechanical compliance to be retrofitted onto our existing snake robots. Modeling and experiments combining the spring with our current snake modules also indicate that this spring should enable a future robot to accurately sense joint torques to within 5% error.

There are several avenues of future work involving these series elastic actuators. A key next step for designing controllers is to characterize the frequency response and impedance of these springs. Other work involves better modeling of the hysteresis and non-linearity of the springs, so that they can be effectively used for force control at higher torques, or so that high-hysteresis rubbers can be used if greater damping is desired. We are currently exploring a wide variety of physical and non-physical hysteresis models [15].

An entire snake robot has been retrofitted with these springs, and tests to characterize its effect on locomotion and system reliability are underway. Unfortunately, our modules are unable to

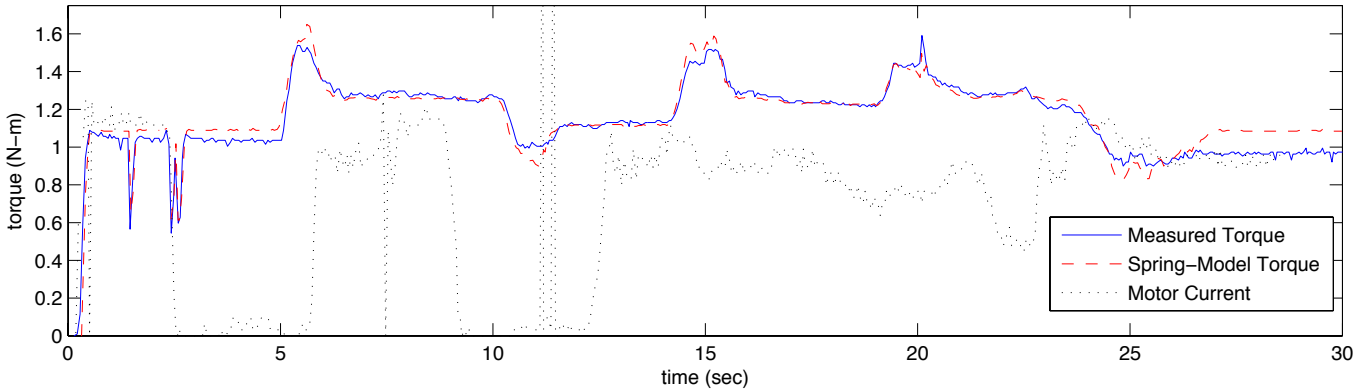

Figure 6: The estimated and actual torque for a trial where a 40A durometer natural rubber elastic element was deflected on a test rig by one of our snake robot modules. The module was commanded to hold a torque while the angular position of the output hub was manually varied. Even though the applied force varied significantly from the commanded value, a simple linear model of the spring's deflection (red dashed line) was able to accurately predict the measured torque (solid blue line), compared to attempts to model the torque based on motor current (black dotted line).

sense the deflection of the springs, and thus be unable to perform torque-control. However, we hope to see other benefits of mechanical compliance, like the reduction of shock load on the robot's gear trains. We are currently building a new snake robot whose modules will be able to measure the deflection of the elastic element to estimate joint torque. We hope that being able to execute torque-controlled gaits in addition to our existing position-controlled gaits will open an exciting new line of research in snake robot locomotion and control.

ACKNOWLEDGEMENTS

The authors would like to thank Andrew Willig, Justin Barsano, Andrew Burks, Anton Galkin, Glenn Wagner, and Mike Stein at MPS Manufacturing. This work was supported by the DARPA M3 program.

REFERENCES

[1] Chirikjian, G., and Burdick, J., 1995. "The kinematics of hyper-redundant robot locomotion". *IEEE Transactions on Robotics and Automation,* **11**(6), pp. 781–793.

[2] Wright, C., Buchan, A., Brown, B., Geist, J., Schwerin, M., Rollinson, D., Tesch, M., and Choset, H., 2012. "Design and Architecture of the Unified Modular Snake Robot". In IEEE International Conference on Robotics and Automation (ICRA), pp. 4347–4354.

[3] Pratt, G., and Williamson, M., 1995. "Series elastic actuators". *Proceedings 1995 IEEE/RSJ International Conference on Intelligent Robots and Systems.*, pp. 399–406.

[4] Hirose, S., 1993. *Biologically Inspired Robots*. Oxford University Press.

[5] Hirose, B. Y. S., and Yamada, H., 2009. "Snake-Like Robots". *IEEE Robotics & Automation Magazine*(March), pp. 88–98.

[6] Yim, M., Shen, W., and Salemi, B., 2007. "Modular self-reconfigurable robot systems". *Robotics & . . .* (March).

[7] Robinson, D. W., Pratt, J. E., Paluska, D. J., and Pratt, G. A., 1999. "Series elastic actuator development for a biomimetic walking robot". In IEEE/ASME International Conference on Advanced Intelligent Mechatronics.

[8] Hurst, J. W., 2008. "The Role and Implementation of Compliance in Legged Locomotion". PhD thesis, Carnegie Mellon University.

[9] Seyfarth, A., Geyer, H., Blickhan, R., and Lipfert, S., 2006. "Running and walking with compliant legs". *Lecture Notes in Control and Information Sciences: Fast Motions in Biomechanics and Robotics,* **340**, pp. 383–401.

[10] Kong, K., Bae, J., and Tomizuka, M., 2010. "A compact rotary series elastic actuator for knee joint assistive system". In IEEE International Conference on Robotics and Automation (ICRA), pp. 2940–2945.

[11] Diftler, M., Mehling, J., Abdallah, M., Radford, N., Bridgwater, L., Sanders, A., Askew, R., Linn, D., Yamokoski, J., Permenter, F., Hargrave, B., Platt, R., Savely, R., and Ambrose, R., 2011. "Robonaut 2-the first humanoid robot in space". In IEEE International Conference on Robotics and Automation (ICRA), Vol. 1, pp. 2178–2183.

[12] Lee, W., 1990. "Designing articulated legs for running machines". PhD thesis, Massachusetts Institute of Technology.

[13] Gent, A. N., 2001. *Engineering with Rubber: How to Design Rubber Components*, 2nd ed. Hanser Publications.

[14] Karlsson, F., and Persson, A., 2003. "Modelling Non-Linear Dynamics of Rubber Bushings - Parameter Identification and Validation". PhD thesis, Lund University.

[15] Kikuchi, M., and Aiken, I. A. N. D., 1997. "An Analytical Hysteresis Model for Elastomeric Seismic Isolation Bearings". *Earthquake Engineering and Structural Dynamics,* **26**, pp. 215–231.